recycling

MDPI

Article

Eco-Audit Comparison of End-of-Life Strategies for Thermoset and Thermoplastic Wind Turbine Blades

Navid Farazmandnia and Adrian Ilinca *

Department of Mechanical Engineering, École de Technologie Supérieure, 1100 Notre-Dame Street West, Montreal, QC H3C 1K3, Canada; navid.farazmandnia.1@ens.etsmtl.ca

* Correspondence: adrian.ilinca@etsmtl.ca

Abstract

Wind turbine blade composites represent a growing end-of-life (EoL) waste challenge because thermoset blades lack commercially mature recycling routes, whereas thermoplastic blades offer improved recyclability through dissolution. This study compares the net environmental impact of ten EoL strategies for six 45 m blade configurations comprising thermoset epoxy and thermoplastic Elium resin systems reinforced with glass fiber, carbon fiber, and hybrid laminates, using an eco-audit methodology based on cumulative primary energy demand. Solvolysis is the leading route for thermoset blades and dissolution for thermoplastic blades, reducing net impact to 74.9%, 31.7%, and 22.4% and to 53.6%, 23.4%, and 18.3% of the landfill benchmark for glass-fiber, hybrid, and carbon-fiber configurations, respectively. Thermoplastic blades therefore fall 296.0, 273.1, and 217.2 GJ below their thermoset counterparts. High-voltage fragmentation, conventional pyrolysis, and microwave-assisted pyrolysis are counterproductive for thermoset glass-fiber blades, exceeding landfill by 26.6%, 18.9%, and 8.1%, respectively, because of high process energy and the limited value of recovered glass fiber. Both material-system selection and recycling-route selection govern end-of-life performance, with the route dimension dominating for glass-fiber blades. A Monte Carlo analysis in which all parameters vary simultaneously confirms that solvolysis and dissolution remain the preferred routes for their respective material systems in every run. Thermoplastic blades fall below their thermoset counterparts in 100.0% and 98.8% of runs for glass-fiber and hybrid laminates, but in 80.3% for carbon fiber, where the advantage is indicated rather than established. These results highlight the importance of designing future wind turbine blades through material selection and recyclable composite systems.

Keywords: wind turbine blades; end-of-life management; thermoplastic composites; eco-audit; dissolution recycling; circular design

Check for updates

Academic Editor: Feihong Guo

Received: 5 August 2026
Revised: 4 September 2026
Accepted: 7 September 2026
Published: 10 September 2026

Copyright: © 2026 by the authors. Licensee MDPI, Basel, Switzerland. This article is an open access article distributed under the terms and conditions of the Creative Commons Attribution (CC BY) license.

1. Introduction

Wind power systems depend on lightweight composite rotor blades; however, the substantial embodied energy (EE) and limited recyclability of fiber-reinforced composites present significant challenges to their long-term sustainability [1]. Larger turbines with longer blades increase energy capture and can reduce the levelized cost of electricity, but they also increase blade material demand and intensify challenges related to manufacturing and end-of-life (EoL) management [1]. As the first generation of modern wind turbines reaches decommissioning, blade disposal and recycling have become major environmental and industrial concerns [2,3]. Increasing blade-waste volumes have strengthened interest

in reuse, recycling, and recovery as practical management routes [4]. Although individual EoL routes have been studied, their results cannot be compared directly when the studies use different blade compositions, system boundaries, process data, and assumptions about the use of recovered materials [5].

Commercial wind turbine blades (WTBs) are predominantly manufactured with thermoset (TS) polyester, vinyl ester, or epoxy matrices reinforced with glass fiber (GF), while carbon fiber (CF) is used more selectively in highly loaded regions such as spar caps [5,6]. GF remains the principal reinforcement in most blade structures, whereas CF is introduced where its higher stiffness can reduce structural mass or control deflection [5]. A hybrid blade combines GF and CF within the same structure, commonly retaining GF across much of the blade and using CF in stiffness-critical regions [1]. This distinction is environmentally and economically relevant because CF can reduce structural mass, but carbon-fiber composites are more expensive than glass-fiber composites and virgin CF is substantially more energy intensive to produce than virgin GF [5]. Thermoset systems are established in blade manufacturing because they provide high specific strength and stiffness, fatigue resistance, and compatibility with the infusion and curing of large structures [7]. Their permanently crosslinked polymer networks, however, cannot be remelted, which limits matrix recovery and makes high-value recycling difficult [4].

Thermoplastic (TP) composites have therefore gained growing research interest as candidate materials for future blade structures [7]. In particular, the low viscosity of liquid acrylic thermoplastic resins such as Elium permits vacuum infusion using processing approaches related to those used for thermoset composites [8]. Unlike permanently crosslinked thermosets, thermoplastic matrices can be softened and reprocessed, and Elium-based composites can be separated by dissolution to recover the polymer and reinforcement [9]. Dissolution studies on acrylate-based thermoplastic composites have also recovered reinforcement for use in second-generation materials [10,11]. Thermoplastic systems may additionally support fusion joining, repair, and alternative recycling routes [7]. These properties create the potential to reduce life-cycle burdens. However, EoL recovery is only one part of life-cycle performance, which is also influenced by material production, manufacturing, transport, and operation [12]. Within the EoL stage, the result depends on process energy and the extent to which recovered materials replace virgin production [13].

Despite these advantages, thermoplastic composites have not been adopted widely in primary commercial blade structures [5]. Research has progressed from laboratory laminates to blade components and selected demonstrators [14]. Barriers to wider adoption include reliable manufacturing of thick composite sections and joints, demonstrated long-term structural durability, and industrial-scale production [5,7]. The same durability evidence is what a new matrix system must accumulate before it can be certified for use in primary blade structures, so the two requirements are linked rather than independent. In addition, uncertainty remains about scalable recovery routes and the EoL environmental performance of thermoplastic blades [5].

The waste hierarchy ranks prevention and service-life extension above reuse and refurbishment, recycling, energy recovery, and landfill [15]. Figure 1 places the EoL routes considered in this study within this hierarchy. This study begins after a blade has been decommissioned and requires EoL treatment. Maintenance, life extension, direct reuse, remanufacture, and refurbishment are outside the system boundary because they postpone or avoid the generation of blade waste. The evaluated pathways are landfill, incineration, cement kiln co-processing, mechanical recycling, high-voltage fragmentation (HVF), dissolution, solvolysis, conventional pyrolysis, microwave-assisted pyrolysis (MAP), and fluidized-bed recycling.

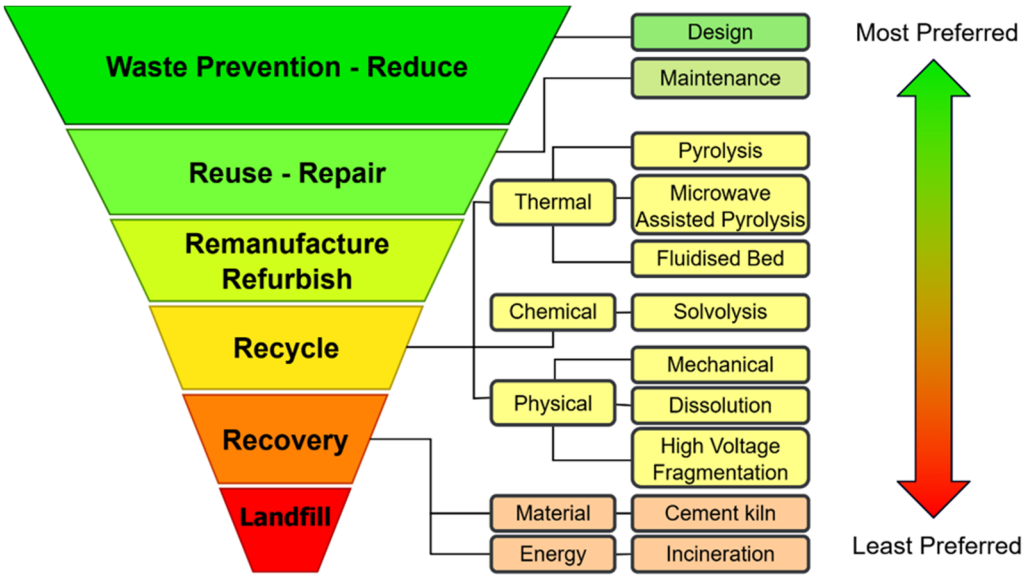


Figure 1. Waste management hierarchy of end-of-life strategies for WTBs. Adapted from [16].

Previous environmental research on blade EoL includes waste-management studies, route-specific life-cycle assessments (LCAs), and comparisons of several recycling processes. Cooperman et al. examined blade-waste quantities, costs, and management options [3], while Nagle et al. compared landfill with cement kiln co-processing [17]. Sproul et al. compared different blade-recycling approaches using LCA [18]. Experimental studies have also examined newer blade-specific processes, including high-voltage fragmentation and microwave-assisted solvolysis [19,20]. For composite waste more broadly, environmental and economic studies have compared mechanical, thermal, and chemical recycling routes for GF- and CF-reinforced materials [13,21,22]. Other assessments have examined CF recovery by pyrolysis and solvolysis [23,24]. Eco-efficiency analysis has also compared alternative carbon-fiber-reinforced polymer (CFRP) recycling technologies [25].

Liu et al. [26] provide the closest prior eco-audit study, comparing eight EoL options for thermoset GF, hybrid GF/CF, and hypothetical CF blade models. Taken together, prior studies have generally focused on one material system, one reinforcement class, or a selected group of EoL technologies [5,18]. Comparative evidence, therefore, remains limited for assessing a broader group of EoL pathways across matched thermoset and thermoplastic blade configurations using the same assumptions [5].

To compare these material systems and EoL routes on a common basis, this study adopts eco-audit as a screening framework. Full LCA evaluates multiple environmental impact categories using detailed inventory data, whereas eco-audit provides an energy-based comparison suited to emerging routes for which complete datasets are unavailable [27]. Techno-economic analysis complements these environmental methods by examining process costs, recovery value, and market competitiveness [28].

Accordingly, this study evaluates ten EoL strategies for six 45 m WTB configurations that combine thermoset or thermoplastic matrices with GF, hybrid GF/CF, or CF reinforcement. The material and geometric definitions of the six blade configurations follow those reported in [12]. This study extends that prior life-cycle comparison by focusing on route-specific EoL processing energy and credits for recovered materials. The objectives are (1) to quantify cumulative primary energy demand for the ten EoL strategies under a consistent eco-audit framework; (2) to identify the lowest modeled primary energy demand for each blade configuration relative to landfill; and (3) to determine whether, and under which assumptions, thermoplastic configurations provide an EoL advantage over their thermoset counterparts. Relative to Liu et al. [26], this study adds thermoplastic blade configurations,

expands the process scope from eight to ten EoL strategies, and tests the robustness of the comparative rankings through one-at-a-time sensitivity tests and a combined Monte Carlo analysis in which 46 parameters vary simultaneously over 100,000 runs. By applying the same accounting rules to all six blade configurations, this study separates the effects of matrix type, reinforcement type, and EoL route.

2. Modeled Results and Sensitivity Analysis

2.1. Net Impact per Blade Configuration and EoL Strategy

Table 1 reports the net primary energy impact of each EoL strategy in GJ per blade, and Figure 2 presents the same results normalized to each configuration's landfill benchmark. Values below 100% indicate a reduction in modeled cumulative primary energy demand relative to landfill, and values above 100% indicate a higher demand.

Table 1. Base-case net primary energy impact (GJ per blade) for ten EoL strategies applied to six blade configurations.

	Thermoset (Epoxy)			Thermoplastic (Elium)		
EoL Strategy	**TS-GF**	**TS-Hybrid**	**TS-CF**	**TP-GF**	**TP-Hybrid**	**TP-CF**
Landfill (benchmark)	891.3	2678.4	4427.5	693.3	2468.4	4237.5
Incineration	839.9	2588.6	4299.4	654.2	2391.0	4121.7
Cement kiln co-processing	789.5	N/A	N/A	614.1	N/A	N/A
Mechanical	791.1	2119.9	3410.6	649.4	1633.6	2611.7
HVF	1128.6	2065.4	2964.3	930.6	1824.8	2713.1
Dissolution	N/A	N/A	N/A	371.5	576.4	775.3
Solvolysis	667.6	849.5	992.5	N/A	N/A	N/A
Pyrolysis	1059.7	1744.9	2392.1	N/A	N/A	N/A
MAP	963.3	1644.2	2287.0	N/A	N/A	N/A
Fluidized-bed	887.8	1517.0	2110.4	N/A	N/A	N/A

Note: Lifetime impact values (GJ/blade, including disposal phase) as previously reported in [12]: TS-GF = 882, TS-Hybrid = 2670, TS-CF = 4420, TP-GF = 684, TP-Hybrid = 2460, TP-CF = 4230. EoL process and recyclate benefit terms are computed per kg of composite and scaled to blade level. N/A = not applicable in this study.

Three factors govern the results and act at different scales. Blade design dominates the absolute values: the lifetime baseline alone ranges from 684 GJ for TP-GF to 4420 GJ for TS-CF, a factor of 6.5, driven by the mass and embodied energy of the reinforcement rather than by any EoL decision. The choice of EoL route moves a given blade by 461 GJ for TS-GF and by up to 3462 GJ for TP-CF, so route selection matters most where the reinforcement is most energy intensive. The material system contributes the smallest of the three: at identical fiber architecture, the thermoplastic blade carries a lifetime impact 190 to 210 GJ below its thermoset counterpart, and this widens to 217 to 296 GJ once the best available route is applied to each. The absolute ranking of the six configurations is therefore determined by blade design, while the improvement achievable within a configuration is set by the route, and the matrix decides which routes are available at all.

All values are calculated using Equation (1). Landfill is used as the benchmark because it represents the lowest-complexity EoL route and provides no material-recovery benefit.

Overall, the base-case results show that solvolysis yields the lowest net impact across all thermoset configurations, whereas dissolution yields the lowest net impact across all thermoplastic configurations. Thermal-route performance varies by reinforcement type, with limited benefit for glass-fiber thermoset blades.

Figure 2 compares all applicable EoL strategies across the six configurations using values normalized to each blade's landfill baseline, which are listed for every strategy and configuration in Supplementary Table S1. Sections 2.2 and 2.3 summarize the thermoset and thermoplastic results, respectively.

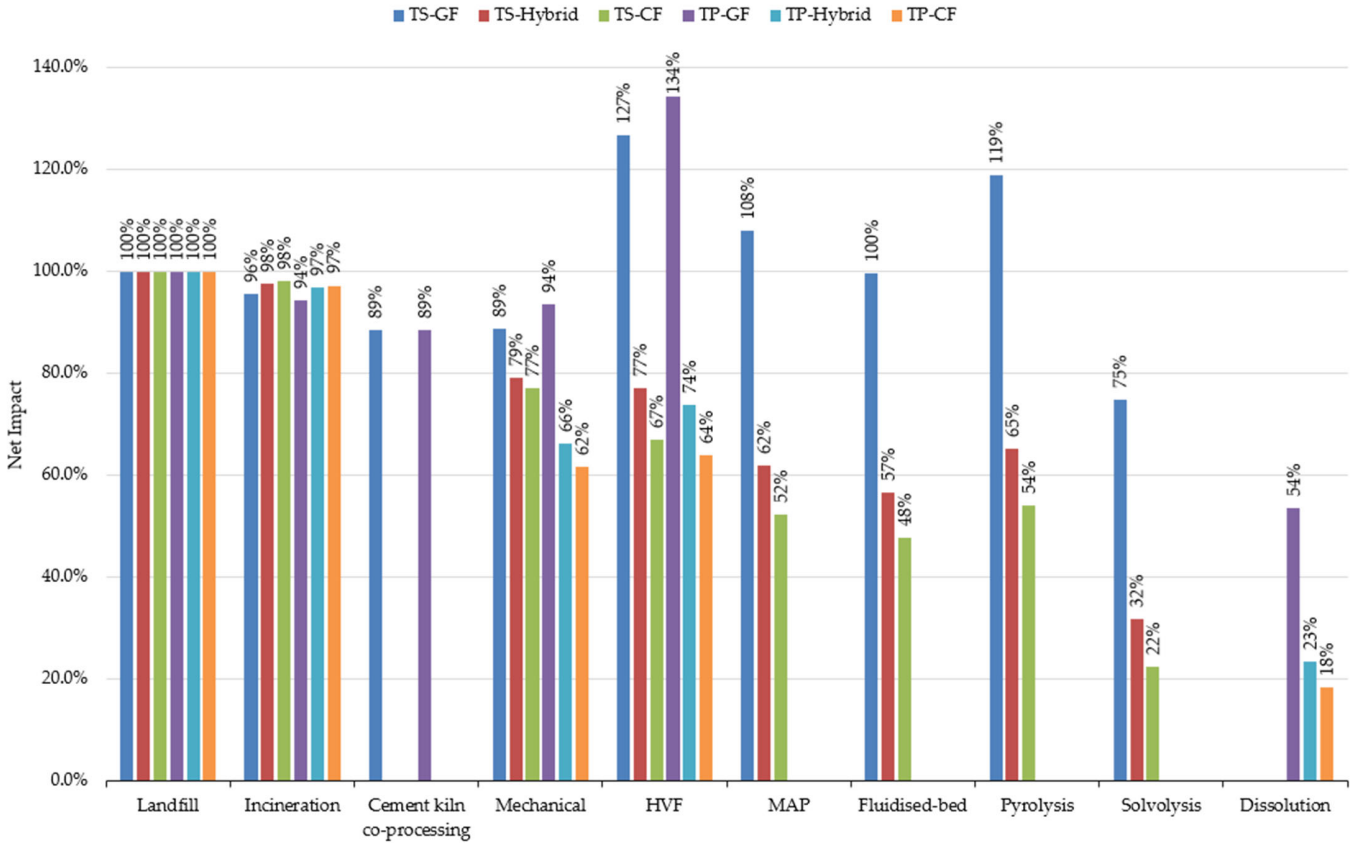


Figure 2. Comparison of net primary energy impact across all six blade configurations and all applicable EoL strategies. Values are normalized to each blade's landfill baseline.

2.2. EoL Performance of Thermoset Blade Configurations

For TS-GF, the lifetime impact dominates the net result. Solvolysis gives the lowest net impact, followed by cement kiln co-processing and mechanical recycling. Because recovered glass fibers have relatively low embodied energy and limited retained tensile strength, the recycling credit is too small to offset the process energy of HVF, pyrolysis, and MAP; these three routes therefore do not improve on the landfill benchmark under base-case assumptions, while fluidized-bed recycling is essentially indistinguishable from it at 99.6% of the benchmark.

For TS-Hybrid, the higher carbon-fiber content increases the value of recovered reinforcement. Solvolysis remains the best-performing route, while thermal recycling becomes more competitive because the recovered carbon-fiber credit increasingly offsets process energy demand. HVF and mechanical recycling provide smaller but still meaningful reductions.

For TS-CF, the high embodied energy of virgin carbon fiber makes high-quality fiber recovery especially important. Solvolysis again gives the lowest net impact, followed by fluidized-bed recycling and MAP, while mechanical recycling is less favorable because lower retained properties reduce the carbon-fiber recyclate credit.

2.3. EoL Performance of Thermoplastic Blade Configurations

For TP-GF, dissolution gives the lowest net impact by a wide margin. Cement kiln co-processing is the next-best route, while mechanical recycling and incineration provide only moderate reductions. HVF exceeds the landfill benchmark by 34.2% at the base-case pulse number, because its process energy is high relative to the credit available from recovered glass fiber.

For TP-Hybrid, dissolution also ranks first because it recovers both high-value carbon fibers and the thermoplastic matrix. Mechanical recycling and HVF provide substantial reductions, with mechanical recycling ahead of HVF by 191 GJ per blade under base-case conditions.

For TP-CF, dissolution again performs best. Mechanical recycling and HVF provide intermediate reductions, while incineration remains ineffective because combustion recovers only a small fraction of the embodied energy in carbon-fiber-dominated composites.

2.4. Robustness of the EoL Rankings Under Uncertainty

The sensitivity analysis assesses the robustness of the EoL rankings to the three classes of uncertainty defined in Section 4.6. Results are presented first for scale-up uncertainty in process energy, then for parameter uncertainty in the recyclate benefit, and finally for the combined probabilistic analysis in which all parameters vary together. Supplementary Figures S1–S3 present the underlying sweeps for the glass-fiber, hybrid, and carbon-fiber configurations, respectively, each showing the process-energy and recyclate-benefit results for the thermoset and the thermoplastic variant of that reinforcement.

2.4.1. Scale-Up Uncertainty in Process Energy

Process-energy uncertainty has little effect on the low-energy routes. Landfill and incineration change net impact by less than 3 GJ per blade across their full ranges, and mechanical recycling by at most 11 GJ. The one consequence is for TS-GF, where cement kiln co-processing and mechanical recycling are separated by only 1.6 GJ per blade at the base case, so the two exchange places at the low bound of the mechanical energy range. Their close ranking for that configuration is not robust.

HVF is the most process-energy-sensitive route. Across the pulse series reported by Mativenga et al. [29], its net impact for TS-Hybrid rises from 2065 to 3436 GJ per blade and falls from fifth to eighth place. For the two glass-fiber configurations, TS-GF and TP-GF, HVF already exceeds the landfill benchmark at the base case, so no point in its energy range yields a net benefit.

Among the lower-maturity thermal routes, MAP is the route whose rank moves. For TS-GF it falls below the landfill benchmark at the low bound of its electrical demand and rises above pyrolysis at the high bound, and for TS-Hybrid and TS-CF it falls one place at the high bound. Fluidized-bed recycling rises above landfill for TS-GF at the upper bound of its process energy. Pyrolysis produces no rank change under variation of its own process energy in any configuration, including when the oxidative cleaning demand defined in Section 4.5.4 is applied at its upper bound of 7 MJ/kg. Solvolysis and dissolution do not change rank at either bound of their own process energy in any configuration, because that energy is small relative to the recyclate credit each generates. The individual rank changes are listed in Supplementary Table S2.

2.4.2. Parameter Uncertainty in the Recyclate Benefit

Virgin carbon-fiber embodied energy is the single most influential parameter in the study. Across its range of 171 to 998 MJ/kg it changes the net impact of solvolysis by 169% of the base-case value for TS-Hybrid and 289% for TS-CF, and of dissolution by 251% and

374% for the corresponding thermoplastic configurations. It also produces the largest single rank change observed: at 171 MJ/kg, HVF falls from fifth to eighth place for TS-Hybrid. Because the parameter is shared by every route, however, it displaces the whole ranking rather than reordering its leading positions.

Among route-specific parameters, fiber yield and retained strength dominate. Mechanical recycling accounts for the largest number of rank changes, followed by HVF and fluidized-bed recycling. Fluidized-bed recycling rises above landfill for TS-GF at the low bounds of its glass-fiber retained strength and yield, and falls from second to fourth place for TS-Hybrid at the lower bound of the carbon-fiber retained strength reported for the process. Mechanical recycling and HVF exchange positions for TP-CF under variation of mechanical fiber yield, mechanical carbon-fiber retained strength, HVF carbon-fiber retained strength, and HVF carbon-fiber yield.

For solvolysis, the retained tensile strength of recovered glass fiber has the widest evidential range of any recyclate parameter in this study, from 0.318 to 0.67, yet it changes the net impact of solvolysis for TS-GF by only 11.4% and produces no rank change. The resin quality factor and resin yield rate affect magnitude but not order in every configuration. For dissolution, the resin quality factor, the resin yield rate, and the retained strength of both reinforcements likewise affect magnitude without altering the ranking. Supplementary Figure S4 ranks the parameters entering solvolysis by the swing each produces, and Supplementary Figure S5 does the same for dissolution.

Across the 49 parameter variations that reorder a configuration, none involves solvolysis or dissolution. The changes are confined to mechanical recycling, HVF, MAP, fluidized-bed recycling, pyrolysis, incineration, and cement kiln co-processing, which are the routes whose base-case values lie closest together. The complete list is given in Supplementary Table S2.

2.4.3. Combined Probabilistic Analysis

When all 46 parameters vary simultaneously, solvolysis achieves the lowest net impact throughout the 100,000 runs for all three thermoset configurations, and dissolution does so throughout the runs for all three thermoplastic configurations. No other route attains the leading position in any run. Table 2 reports the margin by which the leading route falls below the best alternative available to the same blade. It is positive in every run, and its smallest value across all 100,000 runs is 47.3 GJ per blade for TS-GF and 140.6 GJ per blade for TP-GF.

Table 2. Robustness of the leading EoL strategy for each blade configuration under combined variation of all 46 parameters (100,000 draws). The margin is the amount by which the leading route falls below the best alternative available to the same configuration within the same draw.

Blade Configuration	Leading Strategy	Base-Case Margin (GJ)	Margin, 5th Percentile (GJ)	Smallest Margin in 100,000 Draws (GJ)	Probability of Ranking First (%)
TS-GF	Solvolysis	121.9	93.5	47.3	100.0
TS-Hybrid	Solvolysis	667.5	407.8	239.7	100.0
TS-CF	Solvolysis	1117.9	557.8	279.9	100.0
TP-GF	Dissolution	242.6	197.7	140.6	100.0
TP-Hybrid	Dissolution	1057.2	473.3	280.3	100.0
TP-CF	Dissolution	1836.4	676.7	329.5	100.0

A positive margin in every run means the leading route is never displaced. Percentiles are of the margin, not of the net impact of the route. Rank changes among the remaining strategies under one-at-a-time variation are listed in Supplementary Table S2.

The percentile intervals of individual routes nevertheless overlap for the hybrid and carbon-fiber configurations. For TS-Hybrid, solvolysis spans 30.5% to 70.7% of the landfill benchmark between the fifth and ninety-fifth percentiles while fluidized-bed recycling spans 59.3% to 87.4%. This overlap does not indicate a fragile ranking. It arises because the parameters of largest influence, principally the embodied energies of the virgin materials and the primary energy factors, are shared by every route and displace them together within each run, so the marginal distribution of a single route overstates the uncertainty in its position relative to the others.

The comparison that matters most to this study is between material systems rather than within one, because the leading route differs between them: dissolution is available only to the thermoplastic blades and solvolysis only to the thermosets. Table 3 reports, for each reinforcement type, the margin by which the best thermoplastic option falls below the best thermoset option in the same run. For glass fiber the thermoplastic blade is lower in 100.00% of runs, by at least 98.6 GJ per blade. For the hybrid laminate it is lower in 98.84% of runs. For carbon fiber the proportion falls to 80.33%, and the fifth percentile of the margin is negative at −149.3 GJ per blade, meaning that about one in five runs the thermoset blade recycled by solvolysis outperforms the thermoplastic blade recycled by dissolution.

Table 3. Comparison between material systems under combined variation of all 46 parameters (100,000 runs). The margin is the amount by which the best thermoplastic option falls below the best thermoset option for the same reinforcement within the same run; a positive value means the thermoplastic blade has the lower net impact.

Reinforcement	Base-Case Margin (GJ)	Margin, 5th Percentile (GJ)	Median Margin (GJ)	Smallest Margin in 100,000 Runs (GJ)	Runs in Which the Thermoplastic Blade Is Lower (%)
Glass fiber	296.0	213.7	275.7	98.6	100.00
Hybrid	273.1	65.6	223.8	−206.3	98.84
Carbon fiber	217.2	−149.3	138.9	−613.4	80.33

Dissolution is the best thermoplastic option and solvolysis the best thermoset option in every run, so the comparison is equivalent between those two routes. A negative fifth percentile indicates runs in which the thermoset blade performs better.

The reinforcement masses reported in Table 4 help explain this result. The embodied energy of virgin carbon fiber is the most influential parameter in this study, and it affects both material systems.

Table 4. Bill of materials of the six WTB variants considered in this study, in kilograms per blade [12].

Name	Materials	TS-GF	TS-Hybrid	TS-CF	TP-GF	TP-Hybrid	TP-CF
Glass Fiber Unidirectional	S-glass	2414	1207	-	2414	1207	-
Glass Fiber Biaxial/Triaxial	E-glass	3084	1542	-	3084	1542	-
Carbon Fiber	-	-	1924	3848	-	1924	3848
Thermoset Resin	Epoxy	2940	2940	2940	-	-	-
Thermoplastic Resin	Elium 188 XO	-	-	-	2940	2940	2940
Mass excluded from EoL processing	Metals, balsa, PVC, VARTM consumables, and other minor materials	1055	1055	1055	1055	1055	1055
Total weight (kg)	**-**	**9493**	**8668**	**7843**	**9493**	**8668**	**7843**

The thermoplastic advantage also depends on recovery of the Elium matrix and on a lower lifetime baseline, neither of which scales with reinforcement content. As the carbon-fiber content increases, the shared fiber credit grows relative to these two advantages, narrowing the margin between the material systems. The conclusion that thermoplastic blades achieve a lower end-of-life primary energy demand is therefore established for glass-fiber and hybrid laminates within the parameter ranges assessed here, but is indicated rather than established for carbon-fiber laminates.

Discrete scenarios confirm the within-system pattern with one exception. Adopting the pressure-swing distillation flowsheet for dissolution, which raises its process energy fivefold and its resin yield to 0.90, leaves dissolution the leading thermoplastic route in all three configurations at 568, 773, and 972 GJ per blade. Varying the electricity primary energy factor between 2.1 and 3.6 changes no leading route, because neither solvolysis nor dissolution is electricity intensive. Setting every parameter simultaneously to its least favorable bound leaves solvolysis and dissolution leading in all six configurations. The exception is the process scale adopted for solvolysis: substituting the laboratory-derived value of 38.4 MJ/kg reported by Meng et al. [5] for the industrial-scale value of Lahive et al. [30] raises solvolysis for TS-GF to 844 GJ per blade and makes cement kiln co-processing the leading route for that configuration at 790 GJ per blade, while leaving TS-Hybrid and TS-CF unaffected. This is the quantitative justification for adopting an industrial-scale value, since a laboratory batch figure for one route alone would reintroduce the scale inconsistency that the process-energy basis adopted in this study is intended to avoid.

The rank changes summarized above are listed in full in Supplementary Table S2. Table 2 reports the robustness of the leading strategy in each configuration.

3. Discussion and Limitations

That crosslinked thermosets cannot be remelted, whereas thermoplastic matrices can be remelted or dissolved, is well established and is not offered here as a finding. What this study establishes is whether, and under which assumptions, that potential translates into a lower modeled end-of-life primary energy demand: the two material systems are compared on a single set of recyclate-quality and functional-substitution rules (Section 4.5), a single scale-up treatment applied by technology readiness level (Section 4.6), and the same recovery burdens, including the size-reduction deduction and oxidative post-processing where it applies (Sections 4.2 and 4.5.4).

Across all six configurations, the net primary energy impact is governed largely by the lifetime baseline before EoL credits are applied. The landfill benchmark is lowest for TP-GF and highest for TS-CF, reflecting the influence of blade design and material selection. Carbon-fiber blades, therefore, retain higher total impacts than glass-fiber blades even when favorable EoL routes are used.

Overall, EoL benefit depends on the interaction between blade design, process energy, and avoided burden. Lifetime impact sets the overall magnitude, while EoL ranking depends on whether the recovered-material credit is sufficient to offset the energy required for recycling.

3.1. Dissolution as a Transformative Route for Thermoplastic Blades

The most significant finding of this study is the substantial reduction in modeled cumulative primary energy demand achieved by dissolution for thermoplastic blades, especially TP-GF. Its performance is explained by three linked factors:

First, dissolution has a low process energy of 6.31 to 7.85 MJ/kg depending on resin fraction, comparable to solvolysis and substantially below pyrolysis, MAP, fluidized-bed recycling, and HVF.

Second, dissolution recovers both reinforcement fibers and the Elium matrix in reusable form. This provides a matrix credit absent from thermal recycling routes.

Third, glass fibers recovered from Elium composites by dissolution retain full tensile strength, much higher than that of glass fibers recovered by thermoset solvolysis, and carbon fibers retain 95.8% of virgin strength [8,31], maximizing the fiber credit.

Dissolution nevertheless remains a pilot-scale route. Solvent recovery is included in the adopted process energy, which is derived from a facility-scale model rather than a laboratory batch, but solvent management and the safety issues associated with volatile solvents such as acetone remain to be resolved at the industrial scale before dissolution is considered commercially mature.

3.2. Thermal Recycling Strategies for Thermoset Blades

Thermal recycling results are governed by the balance between process energy and the avoided burden of recovered reinforcement. This balance favors carbon-fiber-rich waste streams more than glass-fiber waste streams because recovered carbon fiber carries a much larger avoided embodied-energy credit.

MAP results, especially for TS-GF and TS-Hybrid, remain indicative because the adopted process-energy value comes from a single automotive CFRP recycling study [32] rather than blade-scale glass-fiber or hybrid laminates.

Fluidized-bed recycling is modeled here in its conventional form, without the fiber-regeneration step that has been reported to restore a substantial part of the tensile strength of thermally recovered glass fiber. Regeneration would raise both the process energy and the recyclate credit, and it represents a plausible route to improving the glass-fiber balance that is not yet reflected in blade-scale inventories. This reinforcement-dependent pattern is consistent with previous eco-audit work showing that thermal recycling is more favorable for carbon-fiber configurations than for glass-fiber thermoset blades [26].

3.3. Limitations

Several limitations of the present study should be acknowledged.

The EoL stage is modeled with a gate-to-gate boundary, while transportation and disposal preparation remain embedded in the lifetime baseline. Published recycling inventories differ in whether they include these operations, so adding them to some routes and not others would break the common accounting basis. Its magnitude was nevertheless calculated rather than assumed negligible. The magnitude is bounded directly. Liu and Barlow [1] report 0.46 MJ per tonne-kilometer for a 32-tonne truck, and note that a blade requires such a truck because of its size and that a truck carries one blade at a time, giving 14.72 MJ per blade-kilometer by road. Applying the 25 km wind-plant-to-landfill distance modeled by Cooperman et al. [3] gives 0.37 GJ per blade, which is 0.8% of the smallest margin separating a leading route from its best alternative in Table 2. Only the difference in distance between routes could affect a ranking, and it is smaller still. Route-specific transport, inter-facility logistics, and geographic access to specialized recycling infrastructure are therefore outside the scope of this comparison. The supporting calculation is given in Supplementary Methods S2.

The eco-audit methodology evaluates cumulative primary energy demand as a single aggregated metric. Although carbon footprints could, in principle, be evaluated within the same framework, consistent CO_2-equivalent datasets are not currently available for all ten EoL strategies examined. Furthermore, energy-based metrics cannot capture potential burden shifting between environmental categories such as acidification, toxicity, freshwater consumption, particulate emissions, or residual waste generation. Addressing these aspects would require a full multi-category LCA.

The eco-audit methodology is intended as a screening and comparative decision-support tool rather than a replacement for a full life-cycle assessment compliant with ISO 14040 and 14044. Its principal strength lies in enabling consistent comparison of multiple recycling technologies, including emerging processes for which comprehensive life-cycle inventory data are not yet available. Consequently, the methodology is particularly well suited to identifying promising end-of-life pathways during the early stages of technology development, while more detailed multi-impact LCAs can subsequently be undertaken as process-specific inventory data become available.

Several process energy values and recyclate benefit parameters for thermoplastic blade configurations were adopted from thermoset equivalents because primary experimental data were unavailable, particularly for HVF process energy and mechanical recycling yield. Section 4.5 discusses the physical justification for these assumptions. Each parameter carries an assumed uncertainty in the sensitivity analysis, and none alters the leading route in any configuration, although several contribute to rank changes among the remaining strategies listed in Supplementary Table S2. Nevertheless, future experimental studies specifically addressing Elium-based composites would substantially reduce uncertainty.

The process energy values of Table 5 are drawn from industrial-scale facility models and plant inventories, whereas the recovery parameters of Tables 6 and 7 rest on laboratory- and bench-scale measurements, because no blade-scale recyclate characterization has been published for most routes. This asymmetry is accepted here on the grounds that recyclate quality is a material property and is far less scale-dependent than energy intensity, but it should be borne in mind when the absolute magnitudes are interpreted. A related asymmetry applies within Table 6: the retained strength ratios for mechanical recycling of thermoplastic configurations are second-generation composite ratios, while those for the thermoset configurations and for the thermal and chemical routes are single-fiber or component-level ratios.

The techno-economic dimension of EoL strategy selection remains outside the scope of the present study. Environmentally favorable recycling routes may not yet be economically viable under current industrial conditions. Dissolution infrastructure for Elium composites remains at pilot scale, while solvolysis has not yet reached commercial deployment for WTB applications.

Equation (3) implicitly assumes that recovered resin displaces virgin resin production in proportion to its assigned quality factor, and Equation (2) makes the same assumption for fiber. The secondary applications realistically available to the recovered materials are narrower than that. Fiber recovered by mechanical recycling and by HVF is short, of mixed length, and partly resin-bonded, and its established uses are as reinforcement in molding compounds, non-structural panels, and cementitious products rather than in new blade laminates. Fiber recovered by the thermal and chemical routes is cleaner and longer and has been demonstrated in structural molding compounds and in non-woven mats, but not in primary blade structures. Recovered epoxy behaves as an inert filler rather than a fully reactive matrix constituent above approximately 10 wt% incorporation [33], and recovered Elium has so far been demonstrated only at loadings up to 5 wt% in a second-generation laminate [34]. Both should therefore be read as lower-grade secondary materials with constrained reuse pathways rather than as direct functional equivalents of their virgin counterparts. This reflects a broader constraint of the eco-audit framework, which assigns recyclate benefits through simplified mass- and energy-displacement relationships without accounting for the secondary material's performance in its subsequent application. The credits computed here therefore represent the primary energy displaced if the recyclate substitutes virgin material at the modeled quality, not a demonstrated closed loop back into blade manufacture. A more rigorous treatment would require integrating recyclate

quality characterization and secondary-product performance assessment into a full life-cycle modeling framework.

A further constraint applies to the retained tensile strength ratios of Table 6 and, through them, to every recyclate credit computed in this study. The avoided-burden formulation assumes that recovered fiber displaces virgin fiber in proportion to its retained strength, but the measured ratios are not free of the way the measurement was made. Three effects are visible in the sources adopted here. First, the reference against which recyclate is compared is rarely controlled. Lester et al. [35] report two virgin baselines in the same table, an experimental value of 4.09 GPa and a manufacturer's datasheet value of 4.5 GPa, which differ by 10% and shift the retained strength ratio of fluidized-bed carbon fiber from 0.75 to 0.68 depending on which is chosen. Second, the measurement protocol itself alters the result: Palmer [36] measured retained strength ratios of 0.827, 0.785, and 0.705 for the same mechanically ground glass fiber at gauge lengths of 5, 10, and 15 mm. Third, and least intuitively, cleaner recyclate can test weaker. Kao et al. [37] attribute the highest retained strength in their series to the sample that retained the most residual resin, which acted as a protective coating, and Cunliffe et al. [38] measured higher strengths for char-coated fibers separated physically (0.53 to 0.67) than for the same fibers after oxidative cleaning (0.35 to 0.52). Recovered material from HVF carries 32% to 37% residual resin by weight [29]. Retained tensile strength is therefore a partial descriptor of substitution potential. It captures neither fiber length and its distribution, nor surface condition and sizing, nor the interfacial adhesion the recyclate would develop in a new laminate, and the measured value itself depends on the reference, the protocol, and the residual matrix. It is used because it is the only property reported consistently enough across the ten routes to support a common comparison, and the credits computed from it should be read as first-order estimates rather than as demonstrated substitution ratios.

Relatedly, the analysis does not account for composite degradation over the blade's service life, so the recyclate is implicitly compared against a newly manufactured reference rather than material that has spent two decades in operation. This is a gap in the available literature rather than a modeling choice. Almost no recyclate study reports properties against an aged reference, and where a comparison is attempted, the baselines are not controlled between laboratories: Cousins et al. [8] found their second-generation panel substantially stronger than a panel produced by another group and attributed the difference to shorter fibers in the comparator rather than to any property of the recyclate. The direction of the resulting bias is not determinate. Comparing recyclate against new rather than aged material understates its relative performance, while the second-generation composite ratios adopted for the thermoplastic mechanical recycling entries in Table 6 already embed one processing cycle that the single-fiber ratios of the other routes do not. Resolving this would require characterization of recyclate against aged reference material, which does not yet exist for wind turbine blade composites.

Consequently, the rankings should be interpreted as comparative screening results intended to guide future experimental and full life-cycle assessments rather than definitive predictions of industrial performance.

4. Materials and Methods

The environmental performance of wind turbine blade EoL strategies is assessed using the eco-audit methodology [39], a simplified LCA approach based on cumulative primary energy demand per unit mass.

4.1. Assessment Framework

In the present study, process inputs are expressed in MJ/kg of composite waste and scaled to the laminate mass of each blade configuration to report final results in GJ/blade. This enables direct full-blade comparison while retaining the energy-intensity values reported in the source literature.

The net primary energy impact of each EoL scenario is calculated as:

$$\text{Net impact} = \text{Lifetime impact} + \text{EoL processing impact} - (B_{\text{fiber}} + B_{\text{resin}}) \quad (1)$$

where B_{fiber} and B_{resin} are the recyclate benefits, expressed in MJ per kilogram of the original reinforcement and of the original matrix, respectively. Following the avoided-burden approach commonly used in comparative blade-waste assessments [17,40], the lifetime impact comprises material production, manufacturing, transportation from the manufacturing factory to the wind farm, operation and maintenance, and disposal contributions reported in [12]; the EoL processing impact corresponds to the process energy required to recycle or dispose of one kilogram of composite waste entering the facility; and the recyclate benefit comprises two avoided embodied energy terms. B_{fiber} represents the avoided EE associated with recovered reinforcement fibers, while B_{resin} represents the avoided EE associated with recovered matrix material, where applicable. For recycling routes that do not recover the matrix in usable form, including pyrolysis, fluidized-bed recycling, MAP, mechanical recycling, and HVF, B_{resin} is zero.

4.2. System Boundary

The system boundary is gate-to-gate and covers only EoL processing and avoided production of displaced virgin materials. Blade collection, on-site disassembly and size reduction, material separation and sorting, and transportation to the EoL facility are excluded from the EoL processing term because they are already captured in the lifetime disposal baseline reported in [12]. This exclusion applies to the energy of those operations, not to their material consequences. Material lost during size reduction never reaches the recovery step and therefore cannot displace virgin production, so it is carried into the recyclate benefit through the yield rates defined in Section 4.5.

Oxidative post-treatment to remove char from thermally recovered fibers is not excluded by default. Its energy is already captured in the adopted value for fluidized-bed recycling, which oxidizes the matrix and residual char in the same operation, and is carried as an explicit sensitivity parameter for conventional pyrolysis. The treatment of each route is set out in Section 4.5.4.

4.3. Blade Configurations and Lifetime Impact

Six full-scale 45 m WTB configurations are evaluated in this study based on the life-cycle assessment reported in [12]: TS-GF, TS-Hybrid, TS-CF, TP-GF, TP-Hybrid, and TP-CF. These variants combine thermoset epoxy or thermoplastic Elium matrices with glass fiber, carbon fiber, or glass/carbon hybrid (Hybrid) reinforcement, spanning the architectures used in commercial blades of this scale from all-glass to all-carbon, with a hybrid laminate in which carbon replaces glass in the spar cap. Holding the resin mass constant at 2940 kg across all six configurations isolates the effect of reinforcement type, while pairing each thermoset variant with a thermoplastic counterpart having an identical fiber architecture isolates the effect of the matrix type. The lifetime impacts, masses, functional unit of one blade, and system boundary are taken unchanged from the same assessment [12], so the EoL results reported here are directly additive to that baseline rather than reconciled across differing assumptions.

Table 4 separates the fiber-reinforced laminate considered in the EoL calculation from materials outside this boundary. The laminate fraction includes reinforcement fibers and resin. Metals, balsa, and polyvinyl chloride (PVC) foam are assumed to be separated before treatment, while consumables used in vacuum-assisted resin transfer molding (VARTM) are excluded because they are not part of the blade waste stream.

4.4. EoL Environmental Impacts

This study evaluates ten EoL strategies for WTB composites: landfill, incineration, cement kiln co-processing, mechanical recycling, HVF, dissolution, solvolysis, conventional pyrolysis, MAP, and fluidized-bed recycling. Reported processing energies were converted to MJ/kg of composite waste. Sources differ in what they report. Some give the electricity and fuel that a process consumes at the plant, and others give the primary energy needed to generate and deliver that supply. All values in this study are expressed on the primary basis. Where a source reported consumption at the plant, it was converted using factors of 2.5 for electricity and 1.1 for natural gas, applied identically to every route so that all ten strategies rest on one accounting basis. Detailed process descriptions, source-selection criteria, and derivations are provided in Supplementary Methods S1. Adopted values are summarized in Table 5.

4.4.1. Landfill

Before landfill disposal, blade sections require shredding and size reduction for transport, handling, and burial. A primary energy demand of 1.1 MJ/kg of composite waste is adopted for landfill operations [5]. Size reduction is not included in this value because it is already captured in the lifetime disposal baseline, and the same value is applied to all configurations.

4.4.2. Incineration

Incineration is modeled as co-combustion with municipal solid waste in a combined heat and power facility [41]. Representative gross calorific values are 32 MJ/kg for epoxy resin, 25 MJ/kg for poly(methyl methacrylate)-based thermoplastic resin, and 32.8 MJ/kg for carbon fiber [8,42,43]. A gross process energy of 1.7 MJ/kg is adopted [5]. Of the calorific value released, 13% is delivered as electricity and 25% as heat. Each output is credited as the primary energy it displaces, so the avoided burden is $0.13 \times 2.5 + 0.25 \times 1.1 = 0.60$ MJ for every MJ of calorific value contained in the waste. Glass fibers are non-combustible and receive no energy credit. The credited products are electricity and heat delivered to the grid and to a district heat network, and the displaced background processes are average grid electricity and natural gas heat supply, valued at the same primary energy factors applied to every process energy in this study. No credit is taken for the mineral residue [44]. Combustion emissions are outside the single-indicator scope defined in Section 4.1.

4.4.3. Cement Kiln Co-Processing

Cement kiln co-processing substitutes fossil fuel with the polymer matrix and incorporates the inorganic glass-fiber fraction into clinker. The route is applied only to TS-GF and TP-GF because carbon fibers do not provide the same mineral-substitution function and may affect clinker chemistry or kiln operation [45]. A gross process energy of 1.3 MJ/kg is adopted [5], and the matrix is credited as a direct substitute for kiln fuel on a primary basis. The resulting net process energies are −10.96 MJ/kg for TS-GF and −8.28 MJ/kg for TP-GF [17,46]. The credited product is kiln fuel displaced by the polymer matrix, and the displaced background process is natural gas supply. The glass fraction substitutes silica-bearing raw meal, for which no energy credit is taken because the substituted material is quarried mineral of negligible embodied energy relative to the fuel term. Clinker chemistry, kiln emissions, and product quality are outside the scope of this assessment.

4.4.4. Physical Recycling

Mechanical recycling reduces composite waste through shredding and milling. A process energy of 0.8 MJ/kg is applied to all configurations, corresponding to industrial grinding with fiber retention [5]. HVF uses short high-voltage pulses to separate composites along fiber–matrix interfaces. Mativenga et al. [29] measured a direct electrical demand of 17.1 MJ/kg on glass-fiber thermoset composite at 500 pulses, rising to 89.1 MJ/kg at 2000 pulses. On a primary basis, the base case is therefore 42.75 MJ/kg, applied to all configurations in the absence of thermoplastic-specific energy data, and the reported pulse range is assessed in the sensitivity analysis. Dissolution physically recovers reinforcement fibers and thermoplastic polymer without degrading the polymer chains; therefore, it is not applicable to thermoset matrices. Cousins et al. [8] report 4.0 MJ/kg for dissolution, solvent recovery, and extrusion of an Elium composite containing 22.1 wt% resin. Because both the solvent inventory and the evaporation duty scale with polymer mass rather than composite mass, this value is rescaled to the resin mass fractions of the present configurations, giving 6.31, 7.00, and 7.85 MJ/kg for TP-GF, TP-Hybrid, and TP-CF, respectively.

4.4.5. Chemical Recycling

Solvolysis cleaves thermoset cross-links using reactive solvents at elevated temperature and pressure. Lahive et al. [30] modeled a 10,000 t/y solvolysis facility processing end-of-life wind turbine blade waste, with solvent recovery inside the system boundary and recovery of the degraded matrix as a usable product. Their inventory is tabulated at four resin-to-fiber ratios, from 10:90 to 40:60, against ratios of 35:65, 39:61, and 43:57 for the configurations of this study, so the process energy is interpolated to each composition rather than rescaled from a single value. This gives 6.1, 6.3, and 6.4 MJ/kg for TS-GF, TS-Hybrid, and TS-CF, respectively. An industrial-scale value is adopted so that every route in Table 5 rests on a comparable production scale.

4.4.6. Thermal Recycling

Conventional pyrolysis, MAP, and fluidized-bed recycling recover reinforcement fibers by decomposing or combusting the thermoset matrix [47,48]. These routes are excluded for thermoplastic configurations because comparable process-energy data are unavailable and lower-energy routes can preserve the thermoplastic matrix. The adopted pyrolysis energy is 32 MJ/kg for all thermoset configurations [5], and the MAP value is 25 MJ/kg, obtained from a reported direct electrical demand of 10 MJ/kg [32]. Fluidized-bed values are 6.35 MJ/kg for TS-GF, 8.02 MJ/kg for TS-Hybrid, and 10.4 MJ/kg for TS-CF. The glass-fiber value is obtained from the foreground inventory reported by Yang et al. [49] for conventional fluidized-bed recycling of blade waste, 2.07 MJ/kg of electricity and 1.06 MJ/kg of natural gas, converted using the primary energy factors defined above. The carbon-fiber value is taken from [5], and the hybrid value is the average of the glass- and carbon-fiber values weighted on the reinforcement masses of Table 4.

Table 5. Process energy requirement for different end-of-life options of WTB composites (primary MJ/kg composite waste, excluding transport).

EoL Option	TS-GF	TS-Hybrid	TS-CF	TP-GF	TP-Hybrid	TP-CF	Source
Landfill	1.10	1.10	1.10	1.10	1.10	1.10	[5,50] (L)
Incineration	−4.99	−10.69	−17.77	−3.53	−9.07	−15.95	[5,41] (D)
Cement kiln co-processing	−10.96	N/A	N/A	−8.28	N/A	N/A	[5,17] (D)
Mechanical	0.80	0.80	0.80	0.80	0.80	0.80	[5,51–53] (L)

Table 5. *Cont.*

EoL Option	TS-GF	TS-Hybrid	TS-CF	TP-GF	TP-Hybrid	TP-CF	Source
HVF	42.75	42.75	42.75	42.75	42.75	42.75	[29] (D)
Dissolution	N/A	N/A	N/A	6.31	7.00	7.85	[8] (D)
Solvolysis	6.10	6.30	6.40	N/A	N/A	N/A	[30] (D)
Pyrolysis	32.00	32.00	32.00	N/A	N/A	N/A	[5,49] (L)
MAP	25.00	25.00	25.00	N/A	N/A	N/A	[32] (E)
Fluidized-bed	6.35	8.02	10.40	N/A	N/A	N/A	[5,49] (D)

Note: Values represent net EoL processing energy per kilogram of composite waste. Transport is excluded from all values. N/A = not applicable (process not considered for that blade variant in this study). Data source legend: L = value taken from a published compilation or review rather than from a new measurement; D = value derived in this study from data reported in the cited source; E = estimate made in this study where no value exists for the material system.

4.5. Recyclate Benefit Parameterization

For material-recovery EoL pathways, excluding landfill, incineration, and co-processing, a recyclate benefit is included as a negative energy term. The benefit represents avoided embodied energy from displacing virgin materials with recovered recyclate.

4.5.1. Proportionality Hypothesis

The recyclate benefit includes a fiber credit and, where the matrix is recovered in usable form, a resin credit. The fiber credit is scaled by the retained tensile strength of the recovered fiber relative to its virgin equivalent. Tensile strength is an incomplete measure of the ability of a recovered fiber to replace a virgin one, which also depends on fiber length and its distribution, surface condition, sizing, interfacial adhesion, and suitability for the intended manufacturing route. It is adopted here for two reasons. It is a principal performance parameter for structural blade laminates and the property most consistently reported across the ten recovery routes compared here, so it is the only basis on which all of them can be placed on a common footing. Earlier eco-audit comparisons of blade EoL options adopt the same proportionality for the same reason [26,28]. The relationship is therefore a modeling assumption rather than an experimentally validated correlation, and its consequences are examined in Section 3.3. Also, a resin quality factor is introduced for possible degradation of recovered resin, as described in Section 4.5.3. The two benefit terms are calculated as:

$$B_{fiber} = E_{virgin,fiber} \times (\text{retained strength ratio}) \times (\text{fiber yield rate}) \quad (2)$$

$$B_{resin} = E_{virgin,resin} \times (\text{resin quality factor}) \times (\text{resin yield rate}) \quad (3)$$

where Bf_{iber} and B_{resin} are the recyclate benefits, expressed in MJ per kilogram of the original reinforcement and of the original matrix, respectively; they enter the net impact of Equation (1) as negative terms after multiplication by the corresponding constituent mass of the blade given in Table 4. $E_{virgin,fiber}$ represents the EE of virgin reinforcement fibers (MJ/kg), the retained strength ratio corresponds to the tensile strength of recycled fibers relative to virgin fibers, and the fiber yield rate represents the fraction of the original reinforcement recovered as usable recyclate. Similarly, $E_{virgin,resin}$ denotes the EE of the virgin matrix material (MJ/kg), the resin quality factor represents the fraction of virgin resin performance displaced by the recovered matrix material, and the resin yield rate corresponds to the fraction of the original matrix recovered as a usable product.

Every recycling route requires one or more size-reduction stages before the recovery process itself, and some material is lost at each stage. No route-specific measurement of this loss is available in the literature. Following Liu et al. [26], a uniform deduction of 5% is therefore applied to all recovered material, and every fiber yield rate reported in Table 7 is the product of the recovery reported by the cited source and this deduction. Applying the same deduction to every route keeps the comparison internally consistent and avoids penalizing any single route. The deduction is a mass term rather than an energy term, so it does not reintroduce the size-reduction energy excluded from the system boundary in Section 4.2.

For thermoset solvolysis, a base-case resin quality factor of 0.68 [33] and a resin yield rate of 0.56 [54] are adopted, whereas for thermoplastic composite dissolution, a resin quality factor of 0.73 [34] and a resin yield rate of 0.81 [31] are adopted. Each is derived in Section 4.5.3. The resin benefit term Bresin is applied exclusively to solvolysis and dissolution, as these are the only EoL routes considered in this study that recover the matrix material in a reusable form. For all other recycling and disposal processes, Bresin = 0.

4.5.2. Embodied Energy of Virgin Materials

The embodied-energy coefficients used to calculate recyclate benefits are taken from the Granta Selector 2025 R1 eco-audit database [55], which is the source used for the lifetime assessment in [12], so the production and avoided-production terms rest on one dataset. For virgin glass fiber, a blade-specific weighted average of 41.4 MJ/kg is used, derived from S-glass (52.7 MJ/kg) and E-glass (32.5 MJ/kg) values weighted by their respective masses (Table 4). The corresponding base-case values for virgin carbon fiber, thermoset epoxy resin, and thermoplastic Elium resin are 959, 125.5, and 86 MJ/kg, respectively.

4.5.3. Resin Recovery

Most solvolysis studies report the resin degradation yield, the fraction of matrix removed from the fiber, which reaches close to 100% under extended processing conditions [54]. That quantity sets an upper bound on the resin yield rate of Equation (3) rather than equaling it, because matrix removed from the fiber may be degraded into products that cannot substitute for virgin epoxy; it is the recovered usable fraction, not the removed fraction, that earns a credit in this study.

The resin quality factor is measured on second-generation composites, that is, on new laminates manufactured with a defined fraction of recovered resin and tested against an otherwise identical laminate made entirely from virgin resin. The studies that report this comparison give flexural strength, so flexural strength is the basis of the resin credit while tensile strength is the basis of the fiber credit. As with the fiber term, this is a partial descriptor: it records one mechanical property of one laminate configuration rather than the full substitution potential of the recovered resin. It is adopted because it is the only measure of second-generation performance reported for either material system.

With thermosets, not all recovered resin can be reused. Wu et al. [33] measured flexural strength retention in epoxy/GF WTB laminates containing solvolysis-recovered epoxy resin. Retention reached 96% at 5 wt% recovered resin and 68% at 20 wt%. Above approximately 10 wt% recovered resin, the recyclate increasingly behaved as an inert filler rather than a fully reactive constituent of the crosslinked epoxy network. Therefore, 0.68 is used as a conservative base-case resin quality factor.

For thermoplastic composites recycled through dissolution, the matrix is recovered as a solid polymer without covalent bond cleavage, but it is recovered in a polymerized form whereas new Elium composites are infused from monomer, so its performance in a second-generation composite must be measured. Youssef et al. [34] measured flexural strength

retentions of 0.73 at 5.0 wt% and 0.60 at 2.5 wt% recovered Elium recyclate, with 7.5 wt% unable to be infused. Retention would normally be expected to fall as the incorporation level rises, as it does for the epoxy system above, and the authors do not account for the opposite trend observed here. To keep the two material systems comparable, the value at the highest loading successfully tested is adopted in both cases, 20 wt% for epoxy and 5.0 wt% for Elium, giving a base-case resin quality factor of 0.73.

Resin Yield Rate

Muzyka et al. [54] reported a directly measured liquid-product yield from the solvolysis of end-of-life epoxy/GF WTB composites. Their mass balance indicates that the epoxy-relevant Ftalan oligomer fraction corresponds to approximately 55.8% of the original resin mass, which is adopted as a base-case resin yield rate of 0.56.

The remaining dissolved organic products are primarily styrene- and polystyrene-derived compounds [54] and cannot reasonably be substituted for virgin epoxy resin in Equation (3). A sensitivity upper bound of 0.80, representing total oligomer recovery, is examined in Section 4.6.

For thermoplastic dissolution, the recovered Elium matrix is assigned a resin yield rate of 81%, measured by mass balance after acetone dissolution of Elium laminates [31].

4.5.4. Post-Processing of Thermally Recovered Fibers

Fibers recovered by thermal routes carry residual char from incomplete matrix decomposition, and this char must be removed by oxidation before the fiber can be reused [56,57]. Whether that energy is already counted depends on the process. Fluidized-bed recycling oxidizes the matrix and the residual char in the same fluidized combustion step, so the cleaning energy is contained in its adopted process energy. Conventional pyrolysis operates under inert conditions and delivers char-coated fiber, so oxidation is a separate downstream operation whose energy is absent from the adopted value.

For conventional pyrolysis this omission is quantified rather than assumed away. An oxidative cleaning demand of 0 to 7 MJ/kg, derived from the conditions reported by Cunliffe et al. [38], is carried as a parameter in the sensitivity analysis, and its effect on the ranking is reported in Section 2.4.1. For MAP the retained strength ratios of Table 6 were measured on fibers that had not been cleaned, so charging a cleaning energy without also raising the retained strength would penalize the route twice.

Some earlier comparisons approximate post-treatment with a generic 10% deduction to the recyclate benefit. That approach is not used here, because it applies an identical penalty to processes whose char burdens differ and because the effect is now represented explicitly for the route to which it applies. Dissolution, solvolysis, HVF, and mechanical recycling do not thermally degrade the matrix and recover fibers without char, so no post-processing term applies to them.

4.5.5. Parameter Transfer Between Material Systems

Tables 6 and 7 combine measurements from both material systems. Most retained-strength values available in the literature are single-fiber tensile tests on fiber recovered from thermoset laminates, because thermoset recycling has been studied for longer. Where a measurement on a thermoplastic composite exists, it is used for the thermoplastic configurations; where none exists, the corresponding thermoset value is transferred and marked T in Tables 6 and 7.

Mechanical recycling is the one route for which the measurement basis itself differs between the two systems. For glass fiber, the adopted ratio is a second-generation composite measurement on thermoplastic glass-fiber scrap [58], and two measurements on an Elium glass-fiber composite bracket it [59]. For carbon fiber, no measurement on an Elium

composite exists, so the ratio is taken from a polyamide 66 composite [60]; only the matrix polymer differs from the system modeled here.

For HVF, the transfer runs in both directions. No thermoplastic-specific tensile strength retention data are available for glass fiber, so the thermoset glass-fiber retention ratio of 0.88 measured by Rouholamin et al. [61] is adopted for TP-GF composites. For carbon fiber, the direction of transfer is reversed, because the retention ratio of 0.83 was obtained on a thermoplastic carbon-fiber composite [62] and is transferred to the thermoset configurations.

For mechanical recycling, fiber yield is governed mainly by comminution intensity and sieve aperture size rather than matrix chemistry. The thermoset glass-fiber yield of 55% [36,63] is therefore used for the thermoplastic configurations, and the thermoset HVF yield of 57% [36] is used as the TP-GF HVF estimate. Schmidt et al. [64] reported particle size distribution and matrix separation purity for thermoplastic glass-fiber-reinforced polymer under HVF, but no fiber yield. For carbon fiber under HVF, a thermoplastic-specific value is available: Roux et al. [62] recovered 60 wt% of a thermoplastic carbon-fiber component as fragments of processable dimension, which corresponds to 62% of the reinforcement once the fiber contents of the initial composite and of the recovered fragments are accounted for. The derivation is given in Supplementary Methods S1.7.4.

For dissolution-based thermoplastic recycling, the process itself recovers essentially all of the reinforcement. Cousins et al. [8] recovered the full glass content of an Elium spar-cap specimen once the measured mass loss was attributed to polymer, and Gebhardt et al. [31] reported a fiber recovery of about 99% for Elium CFRP. The same process recovery is therefore applied to both TP-GF and TP-CF configurations, and the derivation is given in Supplementary Methods S1.7.1.

Tables 6 and 7 summarize the retained tensile strength ratios, resin quality factors, and fiber and resin recovery yields used throughout this study.

Table 6. Retained tensile strength ratio of recycled fibers relative to virgin fibers, and resin quality factor (QF), by EoL process and blade configuration.

EoL Option	GF in TS	CF in TS	GF in TP	CF in TP	Resin QF	Source
Landfill	N/A	N/A	N/A	N/A	N/A	N/A
Incineration	N/A	N/A	N/A	N/A	N/A	N/A
Cement kiln co-processing	N/A	N/A	N/A	N/A	N/A	N/A
Mechanical	0.78 (L)	0.50 (A)	0.33 (M)	0.80 (M)	N/A	[26,58–60,65]
HVF	0.88 (M)	0.83 (T)	0.88 † (T)	0.83 (M)	N/A	[61,62]
Dissolution	N/A	N/A	1.00 (M)	0.958 (M)	0.73 (M)	[8,31,34,66]
Solvolysis	0.58 (L)	0.95 (L)	N/A	N/A	0.68 (M)	[26,33,67–71]
Pyrolysis	0.52 (M)	0.78 (M)	N/A	N/A	0	[38,72,73]
MAP	0.73 (M)	0.80 (M)	N/A	N/A	0	[35,74]
Fluidized-bed	0.50 (M)	0.75 (M)	N/A	N/A	0	[35,75,76]

N/A = not applicable (process not considered for that blade variant). † = value adopted from the thermoset equivalent. Data source legend: M = value experimentally measured in the cited study; L = value taken from a published compilation or review rather than from a new measurement; T = value transferred from a different material system; A = assumption or estimate stated by the cited source. The mechanical GF in TP and CF in TP entries are second-generation composite strength ratios, and the HVF CF entries are component-level ratios; the mechanical CF in TS entry is an author estimate for which no fiber-level measurement exists (Section 4.5.5); all other entries are single-fiber ratios, as identified in Supplementary Methods S1.7.

Table 7. Fiber and resin yield rates for different recycling processes.

EoL Option	GF in TS	CF in TS	GF in TP	CF in TP	Resin	Source
Landfill	N/A	N/A	N/A	N/A	N/A	N/A
Incineration	N/A	N/A	N/A	N/A	N/A	N/A
Cement kiln co-processing	N/A	N/A	N/A	N/A	N/A	N/A
Mechanical	55% (D)	55% (T)	55% † (T)	55% † (T)	N/A	[26,36]
HVF	57% (D)	57% (T)	57% † (T)	59% (D)	N/A	[26,62,77]
Dissolution	N/A	N/A	95% (D)	95% (D)	81% (M)	[8,31]
Solvolysis	95% (A)	95% (A)	N/A	N/A	56% (M)	[26,78]
Pyrolysis	78% (D)	78% (T)	N/A	N/A	0%	[6]
MAP	78% (T)	78% (T)	N/A	N/A	0%	[6]
Fluidized-bed	42% (D)	86% (D)	N/A	N/A	0%	[26,56,75]

N/A = not applicable (process excluded for that blade variant). † = value adopted from the thermoset GF equivalent. Data source legend: M = value experimentally measured in the cited study; D = value derived in this study from data reported in the cited source; T = value transferred from a different material system; A = assumption or estimate stated by the cited source. All yield rates are expressed on a fiber-mass basis and include the 5% size-reduction deduction defined in Section 4.5.

4.6. Sensitivity Analysis

A sensitivity analysis is conducted to assess the robustness of the comparative ranking of EoL options. The parameters are of three kinds and are treated differently. Scale-up uncertainty applies to the process energies of Table 5, which are drawn from facility models and plant inventories for processes at different stages of industrial development. Parameter uncertainty applies to the recovery parameters of Tables 6 and 7, which are measured properties of recovered material. Model-form uncertainty concerns the gate-to-gate boundary, the avoided-burden formulation, and the restriction of the assessment to cumulative primary energy demand as a single indicator; it is not assigned a numerical range and is addressed in Section 3.3.

Process energies are single-point estimates for processes of differing industrial maturity, so their uncertainty is governed by scale-up rather than by measurement error. Ranges are assigned from AACE International Recommended Practice 18R-97 [79], which classifies expected estimate accuracy by the maturity of the underlying project definition, following the practice permitted by the National Energy Technology Laboratory where research-backed uncertainty levels are unavailable [80]. Because the classes describe design estimates rather than material properties, they are applied to process energy alone and reported as scale-up uncertainty. Technology readiness levels are taken from Meng et al. [5]. Where the cited source reports its own span for the same process configuration, that span is used instead of the AACE class.

The recovery parameters of Tables 6 and 7 are material properties, so no cost-estimate class is applied to them. Each range is derived from the source of the corresponding base-case value: the reported scatter where a source gives replicates, or the span of the underlying measurements where several conditions or studies exist. Where only one measurement exists, an assumed uncertainty of plus or minus 15% is applied and identified as such. The embodied energies of the four virgin materials, the two primary energy factors, and the oxidative post-processing demand are shared by every route and are varied once per run rather than independently.

The analysis is extended to a Monte Carlo simulation so that the parameters vary together rather than one at a time. Each of the 46 parameters is assigned a triangular

distribution, with its most likely value at the base case and its limits at the bounds described above. One value is drawn at random from every distribution, the model is evaluated on that set, and the procedure is repeated 100,000 times. Each route, therefore, has a distribution of 100,000 net impacts, summarized by the fifth, fiftieth, and ninety-fifth percentiles and by the proportion of runs in which it achieves the lowest net impact within its blade configuration.

Two margins are reported, each computed run by run. The first is within a blade configuration: the amount by which the leading route falls below the best alternative available to the same blade. The second is between material systems: the amount by which the best thermoplastic route falls below the best thermoset route for the same reinforcement, which is the comparison on which the central claim of this study depends. Coupled parameters that cannot vary independently are examined as discrete scenarios instead, in particular the solvent-recovery flowsheet for dissolution and the process scale adopted for solvolysis. The AACE class assignments, the assumed uncertainty, and the complete parameter list with bounds, data sources, and distributions are given in Supplementary Methods S2 and Supplementary Table S3.

5. Conclusions

This study compared ten EoL strategies for six 45 m thermoset and thermoplastic WTB configurations using a cumulative-primary-energy eco-audit framework. Within the modeled scenarios, solvolysis produced the lowest cumulative primary-energy demand for thermoset configurations, whereas dissolution provided the lowest net impact for thermoplastic configurations.

The results show that EoL performance is governed by the interaction among the blade material system, process energy, and recovered-material credit. Thermal recycling was unfavorable for glass-fiber thermoset blades but became more competitive for carbon-fiber-containing blades because recovered carbon fiber provides a larger avoided-burden credit.

The thermoplastic configurations achieved a lower net impact than their thermoset counterparts in all three reinforcement types at the base case, with the advantage largest for glass-fiber blades and narrowing for carbon-fiber blades, where reinforcement embodied energy dominated the balance. When all parameters were varied simultaneously, solvolysis and dissolution retained the leading position within their respective material systems throughout the 100,000 runs, and rank changes among the remaining strategies were confined to mechanical recycling, HVF, MAP, fluidized-bed recycling, pyrolysis, incineration, and cement kiln co-processing. The advantage of the thermoplastic blade over the thermoset blade was itself robust for glass-fiber and hybrid laminates, holding in 100.0% and 98.8% of runs, but held in only 80.3% of runs for carbon-fiber laminates and is therefore indicated rather than established for that reinforcement. These conclusions apply to the six configurations, ten strategies, system boundary, and parameter ranges evaluated here.

Future work should extend the analysis to multi-indicator LCA, route-specific logistics, experimental data for Elium mechanical recycling and HVF, and the scale-up of low-TRL recycling routes, especially dissolution and solvolysis.

Supplementary Materials: The following supporting information can be downloaded at: https://www.mdpi.com/article/10.3390/recycling11090165/s1, Methods S1: EoL process-energy evidence and derivations; Methods S2: Detailed material and recovery parameter ranges; Table S1: Net impact of each EoL strategy as a percentage of the landfill benchmark; Figure S1: Glass-fiber blade sensitivity results; Figure S2: Hybrid blade sensitivity results; Figure S3: Carbon-fiber blade sensitivity results; Figure S4: Parameter influence on solvolysis; Figure S5: Parameter influence on dissolution; Table S2: Parameter variations that reorder the EoL strategies of a blade configuration; Table S3: Complete list of varied parameters, their bounds, and the basis of each range.

Author Contributions: Conceptualization, N.F. and A.I.; methodology, N.F. and A.I.; software, N.F.; validation, N.F.; formal analysis, N.F. and A.I.; investigation, N.F. and A.I.; resources, N.F. and A.I.; data curation, N.F.; writing—original draft, N.F. and A.I.; writing—review and editing, N.F. and A.I.; visualization, N.F.; project administration, N.F. and A.I. All authors have read and agreed to the published version of the manuscript.

Funding: This work was supported by the Natural Sciences and Engineering Research Council of Canada (NSERC) [grant numbers RGPIN-2019-04220 and RGPIN-2025-04831]. The funding source had no role in the study design, data collection, analysis or interpretation, manuscript preparation, or the decision to submit the article for publication.

Data Availability Statement: The original contributions presented in this study are included in the article/Supplementary Material. Further inquiries can be directed to the corresponding authors.

Acknowledgments: During the preparation of this work, the authors used AI-assisted technologies, Grammarly (www.grammarly.com), to improve formulation and eliminate grammatical errors. After using this tool/service, the authors reviewed and edited the content as needed and take full responsibility for the published article.

Conflicts of Interest: The authors declare no conflicts of interest.

References

1. Liu, P.; Barlow, C.Y. The environmental impact of wind turbine blades. *IOP Conf. Ser. Mater. Sci. Eng.* **2016**, *139*, 012032. [CrossRef]
2. Carnicero, R.; Cano, L.; Cruz, I. Lessons learned from the sustainable recycling process of a wind blade made with a new thermoplastic resin. *J. Phys. Conf. Ser.* **2024**, *2767*, 072008. [CrossRef]
3. Cooperman, A.; Eberle, A.; Lantz, E. Wind turbine blade material in the United States: Quantities, costs, and end-of-life options. *Resour. Conserv. Recycl.* **2021**, *168*, 105439. [CrossRef]
4. Shen, Y.; Apraku, S.E.; Zhu, Y. Recycling and recovery of fiber-reinforced polymer composites for end-of-life wind turbine blade management. *Green Chem.* **2023**, *25*, 9644–9658. [CrossRef]
5. Meng, F.; Hawkin, J.L.; Gast, L.; Job, S.; Ó Brádaigh, C.M.; Cullen, J.M.; Leeke, G.A.; McKechnie, J.; Poulsen, A.K.; Rothman, R. End-of-life management for wind turbines. *Nat. Rev. Clean Technol.* **2025**, *1*, 677–698. [CrossRef]
6. Beauson, J.; Abrahamsen, A.B.; Villadsen, I.B.V.; Peters, L.; Kaesmacher, B.; Canalis, A.; Andersen, T.L.; Kumar, R.; Rojas, M.; Eltzholtz, J. Glass fibers produced with recovered glass fibers from wind turbine blades—Recycling value chain and properties of glass fibers and composites. *Polym. Compos.* **2025**, *46*, 15795–15810. [CrossRef]
7. Mishnaevsky, L., Jr. Sustainable end-of-life management of wind turbine blades: Overview of current and coming solutions. *Materials* **2021**, *14*, 1124. [CrossRef] [PubMed]
8. Cousins, D.S.; Suzuki, Y.; Murray, R.E.; Samaniuk, J.R.; Stebner, A.P. Recycling glass fiber thermoplastic composites from wind turbine blades. *J. Clean. Prod.* **2019**, *209*, 1252–1263. [CrossRef]
9. Cousins, D.S. *Advanced Thermoplastic Composites for Wind Turbine Blade Manufacturing*; Colorado School of Mines: Golden, CO, USA, 2018.
10. Meyer zu Reckendorf, I.; Sahki, A.; Perrin, D.; Lacoste, C.; Bergeret, A.; Ohayon, A.; Morand, K. Chemical recycling of vacuum-infused thermoplastic acrylate-based composites reinforced by basalt fabrics. *Polymers* **2022**, *14*, 1083. [CrossRef] [PubMed]
11. zu Reckendorf, I.M.; Bergeret, A.; Perrin, D.; Lacoste, C.; Morand, K. Valorization of basalt and glass fibres from vacuum infused acrylate-based composites by coupling mechanical and dissolution recycling pathways. *Sustain. Mater. Technol.* **2024**, *41*, e01113. [CrossRef]
12. Farazmandnia, N.; Ilinca, A. Recyclable Wind Turbine Blades: A Life Cycle Analysis. *Materials* **2025**, *18*, 3762. [CrossRef] [PubMed]
13. Wei, Y.; Hadigheh, S. Cost benefit and life cycle analysis of CFRP and GFRP waste treatment methods. *Constr. Build. Mater.* **2022**, *348*, 128654. [CrossRef]
14. Mishnaevsky, L., Jr. Root causes and mechanisms of failure of wind turbine blades: Overview. *Materials* **2022**, *15*, 2959. [CrossRef] [PubMed]
15. Podara, C.; Termine, S.; Modestou, M.; Semitekolos, D.; Tsirogiannis, C.; Karamitrou, M.; Trompeta, A.-F.; Milickovic, T.K.; Charitidis, C. Recent trends of recycling and upcycling of polymers and composites: A comprehensive review. *Recycling* **2024**, *9*, 37. [CrossRef]
16. Environment and Climate Change Canada. Reducing Municipal Solid Waste. Available online: https://www.canada.ca/en/environment-climate-change/services/managing-reducing-waste/municipal-solid/reducing.html (accessed on 15 April 2026).

17. Nagle, A.J.; Delaney, E.L.; Bank, L.C.; Leahy, P.G. A Comparative Life Cycle Assessment between landfilling and Co-Processing of waste from decommissioned Irish wind turbine blades. *J. Clean. Prod.* **2020**, *277*, 123321. [CrossRef]
18. Sproul, E.; Williams, M.; Rencheck, M.L.; Korey, M.; Ennis, B.L. Life cycle assessment of wind turbine blade recycling approaches in the United States. *IOP Conf. Ser. Mater. Sci. Eng.* **2023**, *1293*, 012027. [CrossRef]
19. Diani, M.; Torvi, S.; Colledani, M. Exploiting high voltage fragmentation to enable demand-driven recycling of end-of-life wind blades. *Procedia CIRP* **2024**, *122*, 837–842. [CrossRef]
20. De Fabritiis, V.; Del Bò, A.; Ciucci, G.A.; Griffini, G.; Turri, S. Microwave-assisted catalyzed solvolysis for rapid recycling of wind turbines composites. *Polym. Degrad. Stab.* **2026**, *250*, 112203. [CrossRef]
21. Vogiantzi, C.; Tserpes, K. A comparative environmental and economic analysis of carbon fiber-reinforced polymer recycling processes using life cycle assessment and life cycle costing. *J. Compos. Sci.* **2025**, *9*, 39. [CrossRef]
22. Witik, R.A.; Teuscher, R.; Michaud, V.; Ludwig, C.; Månson, J.-A.E. Carbon fibre reinforced composite waste: An environmental assessment of recycling, energy recovery and landfilling. *Compos. Part A Appl. Sci. Manuf.* **2013**, *49*, 89–99. [CrossRef]
23. Kawajiri, K.; Kobayashi, M. Cradle-to-Gate life cycle assessment of recycling processes for carbon fibers: A case study of ex-ante life cycle assessment for commercially feasible pyrolysis and solvolysis approaches. *J. Clean. Prod.* **2022**, *378*, 134581. [CrossRef]
24. Pillain, B.; Loubet, P.; Pestalozzi, F.; Woidasky, J.; Erriguible, A.; Aymonier, C.; Sonnemann, G. Positioning supercritical solvolysis among innovative recycling and current waste management scenarios for carbon fiber reinforced plastics thanks to comparative life cycle assessment. *J. Supercrit. Fluids* **2019**, *154*, 104607. [CrossRef]
25. Dieterle, M.; Seiler, E.; Viere, T. Application of eco-efficiency analysis to assess three different recycling technologies for Carbon Fiber Reinforced Plastics (CFRPs). *Key Eng. Mater.* **2017**, *742*, 593–601. [CrossRef]
26. Liu, P.; Meng, F.; Barlow, C.Y. Wind turbine blade end-of-life options: An eco-audit comparison. *J. Clean. Prod.* **2019**, *212*, 1268–1281. [CrossRef]
27. Ashby, M.F. *Materials and the Environment: Eco-Informed Material Choice*; Elsevier: Amsterdam, The Netherlands, 2012.
28. Pender, K.; Yang, L. Waste glass fibre composites valorization using the fluidised bed: A global warming potential and economic assessment. *J. Mater. Cycles Waste Manag.* **2025**, *27*, 343–353. [CrossRef]
29. Mativenga, P.T.; Shuaib, N.A.; Howarth, J.; Pestalozzi, F.; Woidasky, J. High voltage fragmentation and mechanical recycling of glass fibre thermoset composite. *CIRP Ann.* **2016**, *65*, 45–48. [CrossRef]
30. Lahive, C.W.; Dempsey, S.H.; Reiber, S.E.; Pal, A.; Stevenson, K.R.; Michener, W.E.; Alt, H.M.; Ramirez, K.J.; Rognerud, E.G.; Lincoln, C.L. Acetolysis for epoxy-amine carbon fibre-reinforced polymer recycling. *Nature* **2025**, *642*, 605–612. [CrossRef] [PubMed]
31. Gebhardt, M.; Chakraborty, S.; Manolakis, I.; Meiners, D. Closed-loop room temperature recycling of Elium CFRPs and its influence on the 2nd generation composite properties. *J. Plast. Technol.* **2020**, *16*, 179–210. [CrossRef]
32. Suzuki, T.; Takahashi, J. Prediction of energy intensity of carbon fiber reinforced plastics for mass-produced passenger cars. In Proceedings of the 9th Japan International SAMPE Symposium, Tokyo, Japan, 29 November–2 December 2005; pp. 14–19.
33. Wu, M.-S.; Jin, B.C.; Li, X.; Nutt, S. A recyclable epoxy for composite wind turbine blades. *Adv. Manuf. Polym. Compos. Sci.* **2019**, *5*, 114–127. [CrossRef]
34. Youssef, R.; von Monkiewitsch, M.; Zeigmann, G.; Manolakis, I.; Wierach, P.; Opitz, S.; Chakraborty, S. Reuse of recovered recyclate from infusible thermoplastic carbon fiber composites to reduce virgin material usage in reprocessed composites. *J. Compos. Mater.* **2026**. [CrossRef]
35. Lester, E.; Kingman, S.; Wong, K.H.; Rudd, C.; Pickering, S.; Hilal, N. Microwave heating as a means for carbon fibre recovery from polymer composites: A technical feasibility study. *Mater. Res. Bull.* **2004**, *39*, 1549–1556. [CrossRef]
36. Palmer, J.A.T. Mechanical Recycling of Automotive Composites for Use as Reinforcement in Thermoset Composites. Ph.D. Thesis, University of Exeter, Exeter, UK, 2009.
37. Kao, C.; Ghita, O.; Hallam, K.; Heard, P.; Evans, K. Mechanical studies of single glass fibres recycled from hydrolysis process using sub-critical water. *Compos. Part A Appl. Sci. Manuf.* **2012**, *43*, 398–406. [CrossRef]
38. Cunliffe, A.; Jones, N.; Williams, P. Pyrolysis of composite plastic waste. *Environ. Technol.* **2003**, *24*, 653–663. [CrossRef] [PubMed]
39. Ashby, M.; Coulter, P.; Ball, N.; Bream, C. The CES EduPack Eco audit tool—A white paper. *Granta Mater. Inspir. Version1* **2009**, *3*, 1–18.
40. Pender, K.; Romoli, F.; Fuller, J. Lifecycle assessment of strategies for decarbonising wind blade recycling toward net zero 2050. *Energies* **2024**, *17*, 3008. [CrossRef]
41. Li, X.; Bai, R.; McKechnie, J. Environmental and financial performance of mechanical recycling of carbon fibre reinforced polymers and comparison with conventional disposal routes. *J. Clean. Prod.* **2016**, *127*, 451–460. [CrossRef]
42. Chase, M.W. *NIST-JANAF Thermochemical Tables*, 4th ed.; American Institute of Physics: Woodbury, NY, USA, 1998.
43. Karuppannan Gopalraj, S.; Deviatkin, I.; Horttanainen, M.; Kärki, T. Life cycle assessment of a thermal recycling process as an alternative to existing cfrp and gfrp composite wastes management options. *Polymers* **2021**, *13*, 4430. [CrossRef] [PubMed]
44. Larsen, K. Recycling wind turbine blades. *Renew. Energy Focus* **2009**, *9*, 70–73. [CrossRef]

45. Schindler, A.K.; Duke, S.R.; Galloway, W.B. Co-processing of end-of-life wind turbine blades in portland cement production. *Waste Manag.* **2024**, *182*, 207–214. [CrossRef] [PubMed]
46. Cameron, C.V.; Spatari, S.; Baxter, J.B.; Creighton, M.A. Life Cycle Assessment to Quantify Global Warming and Human Health–Respiratory Impacts of Using Composites from Waste Wind Turbine Blades as Feedstock for Cement Clinker and Fiberglass Production. *Environ. Sci. Technol.* **2025**, *59*, 21476–21485. [CrossRef] [PubMed]
47. Krochmalny, K.; Wnukowski, M.; Hardy, T.; Czerep, M.; Rusin, M. Characterization of the products from waste wind turbine blades thermal utilization. *J. Ecol. Eng.* **2025**, *26*, 15–27. [CrossRef] [PubMed]
48. Pickering, S.; Turner, T.; Meng, F.; Morris, C.; Heil, J.; Wong, K.; Melendi-Espina, S. Developments in the fluidised bed process for fibre recovery from thermoset composites. In Proceedings of the 2nd Annual Composites and Advanced Materials Expo, CAMX, Dallas, TX, USA, 26–29 October 2015; Volume 2015, pp. 2384–2394.
49. Yang, J.; Meng, F.; Zhang, L.; McKechnie, J.; Chang, Y.; Ma, B.; Hao, Y.; Li, X.; Pender, K.; Yang, L. Solutions for recycling emerging wind turbine blade waste in China are not yet effective. *Commun. Earth Environ.* **2023**, *4*, 466. [CrossRef]
50. Witik, R.A.; Payet, J.; Michaud, V.; Ludwig, C.; Månson, J.-A.E. Assessing the life cycle costs and environmental performance of lightweight materials in automobile applications. *Compos. Part A Appl. Sci. Manuf.* **2011**, *42*, 1694–1709. [CrossRef]
51. Howarth, J.; Mareddy, S.S.; Mativenga, P.T. Energy intensity and environmental analysis of mechanical recycling of carbon fibre composite. *J. Clean. Prod.* **2014**, *81*, 46–50. [CrossRef]
52. Shuaib, N.A.; Mativenga, P.T. Energy demand in mechanical recycling of glass fibre reinforced thermoset plastic composites. *J. Clean. Prod.* **2016**, *120*, 198–206. [CrossRef]
53. Asmatulu, E.; Twomey, J.; Overcash, M. Recycling of fiber-reinforced composites and direct structural composite recycling concept. *J. Compos. Mater.* **2014**, *48*, 593–608. [CrossRef]
54. Muzyka, R.; Sobek, S.; Korytkowska-Wałach, A.; Drewniak, Ł.; Sajdak, M. Recycling of both resin and fibre from wind turbine blade waste via small molecule-assisted dissolution. *Sci. Rep.* **2023**, *13*, 9270. [CrossRef] [PubMed]
55. Ansys. *Granta Selector 2025, R1*; Ansys: Canonsburg, PA, USA, 2025.
56. Meng, F.; McKechnie, J.; Turner, T.; Pickering, S. Energy and environmental assessment and reuse of fluidised bed recycled carbon fibres. *Compos. Part A Appl. Sci. Manuf.* **2017**, *100*, 206–214. [CrossRef]
57. Termine, S.; Naxaki, V.; Semitekolos, D.; Trompeta, A.-F.; Rovere, M.; Tagliaferro, A.; Charitidis, C. Investigation of carbon fibres reclamation by pyrolysis process for their reuse potential. *Polymers* **2023**, *15*, 768. [CrossRef] [PubMed]
58. Moothoo, J.; Bar, M.; Ouagne, P. Mechanical properties of compression moulded aggregate-reinforced thermoplastic composite scrap. *J. Compos. Sci.* **2021**, *5*, 299. [CrossRef]
59. Kumar, V.; Elen, M.; Sushmita, K.; Overman, N.R.; Nickerson, E.; Murdy, P.; Presuel-Moreno, F.; Fifield, L.S. Hygrothermal aging and recycling effects on mechanical and thermal properties of recyclable thermoplastic glass fiber composites. *Polym. Compos.* **2025**, *46*, 4332–4349. [CrossRef]
60. Colucci, G.; Ostrovskaya, O.; Frache, A.; Martorana, B.; Badini, C. The effect of mechanical recycling on the microstructure and properties of PA66 composites reinforced with carbon fibers. *J. Appl. Polym. Sci.* **2015**, *132*.. [CrossRef]
61. Rouholamin, D.; Shyng, Y.; Savage, L.; Ghita, O. A comparative study into mechanical performance of glass fibres recovered through mechanical grinding and high voltage pulse power fragmentation. In Proceedings of the ECCM16-16th European Conference on Composite Materials, Seville, Spain, 22–26 June 2014; pp. 22–26.
62. Roux, M.; Eguémann, N.; Dransfeld, C.; Thiébaud, F.; Perreux, D. Thermoplastic carbon fibre-reinforced polymer recycling with electrodynamical fragmentation: From cradle to cradle. *J. Thermoplast. Compos. Mater.* **2017**, *30*, 381–403. [CrossRef]
63. Sommer, V.; Becker, T.; Walther, G. Steering sustainable end-of-life treatment of glass and carbon fiber reinforced plastics waste from rotor blades of wind power plants. *Resour. Conserv. Recycl.* **2022**, *181*, 106077. [CrossRef]
64. Schmidt, J.; Auer, M.; Grammel, L.; Woidasky, J. Recycling of Thermoplastic Glass Fiber-Reinforced Composites Using High-Voltage Fragmentation. *Chem. Ing. Tech.* **2024**, *96*, 976–986. [CrossRef]
65. Ogi, K.; Nishikawa, T.; Okano, Y.; Taketa, I. Mechanical properties of ABS resin reinforced with recycled CFRP. *Adv. Compos. Mater.* **2007**, *16*, 181–194. [CrossRef]
66. Tschentscher, C.; Gebhardt, M.; Chakraborty, S.; Meiners, D. Recycling of Elium CFRPs for high temperature dissolution: A study with different solvents. In Proceedings of the Symposium Materialtechnik, Clausthal-Zellerfeld, Germany, 25–26 February 2021; pp. 25–26.
67. Oliveux, G.; Dandy, L.O.; Leeke, G.A. Current status of recycling of fibre reinforced polymers: Review of technologies, reuse and resulting properties. *Prog. Mater. Sci.* **2015**, *72*, 61–99. [CrossRef]
68. Shyng, Y.; Ghita, O. Fragmentation analysis of glass fibres recovered from hydrolysis processes. In Proceedings of the 19th International Conference on Composite Materials, Montreal, QC, Canada, 28 July–2 August 2013.
69. Okajima, I.; Watanabe, K.; Sako, T. Chemical recycling of carbon fiber reinforced plastic with supercritical alcohol. *J. Adv. Res. Phys.* **2012**, *3*, 021211.

70. Liu, Y.; Shan, G.; Meng, L. Recycling of carbon fibre reinforced composites using water in subcritical conditions. *Mater. Sci. Eng. A* **2009**, *520*, 179–183. [CrossRef]
71. Jiang, G.; Pickering, S.J.; Lester, E.H.; Turner, T.; Wong, K.; Warrior, N. Characterisation of carbon fibres recycled from carbon fibre/epoxy resin composites using supercritical n-propanol. *Compos. Sci. Technol.* **2009**, *69*, 192–198. [CrossRef]
72. Onwudili, J.; Insura, N.; Williams, P. Autoclave pyrolysis of carbon reinforced composite plastic waste for carbon fibre and chemicals recovery. *J. Energy Inst.* **2013**, *86*, 227–232. [CrossRef]
73. Cunliffe, A.M.; Williams, P.T. Characterisation of products from the recycling of glass fibre reinforced polyester waste by pyrolysis. *Fuel* **2003**, *82*, 2223–2230. [CrossRef]
74. Åkesson, D.; Foltynowicz, Z.; Christeen, J.; Skrifvars, M. Microwave pyrolysis as a method of recycling glass fibre from used blades of wind turbines. *J. Reinf. Plast. Compos.* **2012**, *31*, 1136–1142. [CrossRef]
75. Pickering, S.J.; Kelly, R.M.; Kennerley, J.; Rudd, C.; Fenwick, N. A fluidised-bed process for the recovery of glass fibres from scrap thermoset composites. *Compos. Sci. Technol.* **2000**, *60*, 509–523. [CrossRef]
76. Yip, H.; Pickering, S.; Rudd, C. Characterisation of carbon fibres recycled from scrap composites using fluidised bed process. *Plast. Rubber Compos.* **2002**, *31*, 278–282. [CrossRef]
77. Weh, A. *High Voltage Pulse Fragmentation Technology to Recycle Fibre-Reinforced Composites*; European Commission: Geneva, Switzerland, 2015; Volume 12.
78. Keith, M.J.; Oliveux, G.; Leeke, G.A. Optimisation of solvolysis for recycling carbon fibre reinforced composites. In Proceedings of the European Conference on Composite Materials 17, Munich, Germany, 26–30 June 2016.
79. Association for the Advancement of Cost Engineering (AACE) International. *Cost Estimate Classification System—As Applied in Engineering, Procurement, and Construction for the Process Industries*; AACE International Recommended Practice No. 18R-97; AACE International: Morgantown, WV, USA, 2016.
80. Sam Hughes, S.H.; Turner, M.; Zoelle, A.; Kuehn, N.; Adams, M.; Eggleston, A. *Quality Guidelines for Energy System Studies: Performing a Techno-Economic Analysis for CO_2 Conversion Technologies*; National Energy Technology Laboratory, U.S. Department of Energy: Pittsburgh, PA, USA, 2023; p. 50.

Disclaimer/Publisher's Note: The statements, opinions and data contained in all publications are solely those of the individual author(s) and contributor(s) and not of MDPI and/or the editor(s). MDPI and/or the editor(s) disclaim responsibility for any injury to people or property resulting from any ideas, methods, instructions or products referred to in the content.